SS2023

PPD

Absorption and Diffraction of X-Ray Radiation

Manuel Lippert - Paul Schwanitz

Group 1

Information

Day	24.05.2023
Place	NWII | 2.2.01.489
Supervisor	Harshit Agarwal
Group Nr.	1
Participant	Manuel Lippert (Manuel.Lippert@uni-bayreuth.de)
	Paul Schwanitz (Paul.Schwanitz@uni-bayreuth.de)

Contents

1 Introduction

In the following, we will present our research on X-Ray diffraction, a versatile measurement method applied in various fields, including industrial applications, solid-state physics, and material science. One of the significant advantages of using X-Rays is their smaller wavelength, because of that, with X-Rays it is possible to operate beyond the limit of resolution of optical microscopy. This enables the representation of smaller structures with higher precision. However, constructing X-Ray lenses is a highly complex task due to the limited refractive index of most materials in this spectral range, which is typically close to or slightly below one. Consequently, the indirect method of "X-Ray Diffraction" is preferred.

In this experiment the X-Ray spectrum of different types of foil will be investigated to determine the type of material and the complexes NaCl (Sodium Chloride) and ZrSiO4 (Zircon/Zirconium(IV)Silicate) will be analyzed with the use of the diffraction method.

2 Theoretical background

2.1 X-Rays

2.1.1 General

X-rays are electromagnetic radiation (EM radiation), which is located between UV and γ-rays. radiation and γ-radiation. The typical wavelength range for X-rays ranges from 100 Å to about 0.05 Å.

2.1.2 Generation using an X-ray tube

The X-ray tube consists of a heated cathode and a beveled anode. Electrons emitted from the cathode are accelerated to the anode by a high voltage. There they strike and generate X-rays. The emission spectrum of one of these tubes consists of two parts. The first part is the characteristic radiation, which is characteristic for the used anode material and appear as spectral lines. The second part is the bremsstrahlung, which forms a continuous background. It is independent of the chosen anode material and is characterized by a short-wave limit. Bremsstrahlung is produced by the deceleration of electrons entering the anode. Since electrons enter at all velocities, all wavelengths are produced (continuum). The wavelength of the lower boundary can be calculated by the law of Duane and Hunt law. The characteristic radiation arises, by the penetration of the electron into the anode. There by this, a bound electron is separated from its atom and this free place is occupied again by a higher electron. The higher electron gives its excess energy in the form of characteristic EM radiation.

2.1.3 Generation using an synchrotron

In a synchrotron, electrons are forced into circular orbits by magnetic fields and accelerated there by alternating electric fields. Due to the circular motion the electrons experience a centrifugal acceleration which leads to a loss of energy in the form of EM radiation, or synchrotron radiation (tangential to the direction of motion). At electron velocities close to the speed of light, the radiated energy is in the range of the X-ray spectrum.

In a wiggler/undulator, this phenomenon is used to generate synchrotron radiation. This consists of a series of dipole magnets, which direct electron beam with almost the speed of light alternately upwards and downwards. By the centrifugal forces, which prevail during the change of direction, synchrotron radiation is generated. The difference between wiggler and undulator is that the wiggler generates a continuous spectrum and the undulator a line spectrum. This is achieved by a different design.

2.2 Interaction of X-rays and matter

X-rays can be absorbed/shielded by matter. This provides the basis for X-ray absorption spectroscopy. Crystalline matter or smaller structures can diffract/scatter X-rays. This is the basis for structural analysis, with which the spatial arrangement of atoms in the crystal can be can be investigated.

In medicine, X-rays are used for diagnostics (e.g., bone fractures) or for the treatment of special diseases (irradiation of cancer). In technology X-rays are used in material testing and quality assurance. For science, X-rays are indispensable for investigating the smallest structures.

2.3 Absorption

2.3.1 Absorption law

The reduction of the radiant power $P(x)$ of the X-rays during absorption can be described as follows:

$$P(x) = P_0 e^{-\mu x} \tag{2.1}$$

Here P_0 is the radiant power before absorption, x is the penetration depth and $\mu = \mu_S + \alpha$ the Attenuation coefficient consists of the scattering coefficient μ_S and the absorption coefficient α.

2.3.2 Absorption edges

In the course of the absorption cross-section as a function of the wavelength, jumps are found. These jumps are called absorption edges and are characteristic for the absorption material. The corresponding energies coincide with the ionization energies of the corresponding inner levels. As the wavelength of the X-rays increases, electrons can be ionized from deeper and deeper shellscan be ionized, which leads to an increase in the absorption cross-section. This increases until the ionization limit of the current shell is reached. After that electrons of the next deeper shell can be ionized. But there at first only electrons in the uppermost level can be ionized, which leads to a jump in the absorption cross-section.

2.4 Crystals

A crystal is a solid with a regular arrangement of atoms/molecules. Crystals are very widespread. They are found in salts, minerals and metals. Crystals, or crystalline material is found in the body in the form of minerals, sugars and proteins.

2.4.1 Crystal structure

By crystal structure is meant the totality of the translational lattice and the atomic base. It is useful to know the structure of the material, because it is important for its properties and behavior.

2.4.2 Symmetrie

Symmetry refers to the invariance of an object with respect to certain operations. This means that an object is subjected to a certain operation (e.g. rotation around its own axis) and it has the same properties as before, i.e. it has not changed and is different from the original state.

2.4.3 cubic lattice

Cubic symmetry is the lattice symmetry of a cubic lattice, this has the highest symmetry of all lattices since it is invariant under all symmetries. By cubic lattice is meant a Bravis lattice class which has the same distances and angles between the outer atoms of a lattice cell.

2.4.4 unit cell

The atoms always sit on the vertices of the unit cell (primitive). Additionally, in a cubic or orthorombic system, they may be centered on the outer surfaces (face centered) or centered in the cell (space centered). In orthorombic or monoclinic systems, it is possible that one atom each is still centered on the lower and upper outer surface (base-centered).

2.5 Diffraction of X-rays

Diffraction is a typical processing phenomenon of waves. These waves deviate after a lateral boundary of the wave field from a straight-line propagation and are deflected. deflected. The reason for this is Huygens' principle that every point of a wave front is the starting point for a new elementary wave. starting point for a new elementary wave.

2.5.1 Laue condition

Laue puts the condition that at diffraction one gets constructive interference only if the change of the wave vector at the scattering process corresponds to a reciprocal lattice vector. Thus one receives the direction of the observed diffraction-reflections at a pure crystal-lattice (without impurities).

The distance between two scattering centers is the lattice vector $\vec{R}$. The wave vector of the (scattered) radiation is $(\vec{k'})\vec{k}$. For the path difference it follows:

$$\Delta x = \vec{R} \cdot \left(\frac{\vec{k}}{k} - \frac{\vec{k'}}{k'} \right) \tag{2.2}$$

For constructive interference the following has to be true:

$$\Delta x = m \cdot \lambda \;\; m \in \mathbb{Z} \tag{2.3}$$

In elastic scattering, the wavenumber of the incident and reflected beam is equal:

$$k = k' = \frac{2\pi}{\lambda} \tag{2.4}$$

It follows:

$$\vec{R} \cdot \left(\vec{k} - \vec{k'} \right) = 2\pi m \;\; \text{bzw.} \;\; \exp\left[i\vec{R} \cdot \left(\vec{k} - \vec{k'} \right) \right] = 1 \tag{2.5}$$

The second equation corresponds to the equation of determination of the reciprocal lattice vectors $\vec{K}$:

$$\exp\left[i\vec{R} \cdot \vec{K} \right] = 1 \tag{2.6}$$

Thus the Laue condition follows:

$$\vec{K} = \vec{k} - \vec{k'} \tag{2.7}$$

2.5.2 Bragg condition

If X-rays hit a crystal, a large part will pass through it unhindered, but a small part will be deflected at the atoms. These deflections are very weak and become stronger when they constructively interfere according to the Bragg condition. Bragg's equation represents the constructive interference between two planes and is reads:

$$n\lambda = 2d \sin(\theta) \tag{2.8}$$

Where n is a natural number (diffraction order), λ is the wavelength of the X-rays, d the distance between two parallel grating planes, and θ the angle between the X-ray beam and the grating plane.

2.6 Centered grid

In a centered lattice, in contrast to the primitive lattice which has only lattice points at the corners, there are additional points in the unit cell. One distinguishes between space-centered lattice, where there is another lattice point in the middle of the unit cell.

Thus, there are a total of two atoms in the cell. The lattice vectors of the bcc-lattice (base-centered-cubic) are: $\vec{a} = \frac{a}{2}(-1,1,1)$ $\vec{b} = \frac{a}{2}(1,-1,1)$ $\vec{c} = \frac{a}{2}(1,1,-1)$.

Another centered lattice is the face-centered lattice, where there is another atom in the center of each side face. Thus there are 4 atoms in the unit cell. The lattice vectors of the fcc lattice (face-centered-cubic) are: $\vec{a} = \frac{a}{2}(0,1,1)$ $\vec{b} = \frac{a}{2}(1,0,1)$ $\vec{c} = \frac{a}{2}(1,1,0)$

The last centered lattice is the base centered lattice, which has one atom in the center of the top and bottom side. There are a total of 2 atoms in the unit cell. The lattice vectors of the base centered orthorombic lattice are: $\vec{a} = (0,0,c)$ $\vec{b} = \left(\frac{a}{2}, \frac{b}{2}, 0\right)$ $\vec{c} = \left(-\frac{a}{2}, \frac{b}{2}, 0\right)$

The centered Bravis grating causes destructive interference of the additional atom. This occurs when, of the Miller/Laue indices hkl, the sum of h and k is odd.

2.7 Powder Diffraction Chart

A peak in the powder diffractogram can be identified by its shape (profile), its position (2θ), and its area (intensity). From the peak positions (2θ), the lattice plane spacing of the crystal can be determined. The intensities can be used to determine the arrangement of the atoms on a lattice plane (thus the Bravis lattice) can be determined.

2.7.1 Atomic form factor and structure factor

The atomic shape factor is a measure of the angular dependence of the intensity of the scattered radiation. It reflects the number of electrons involved in the scattering under a certain angle. The structure factor now includes the interaction of all atoms in the unit cell and reflects the total diffraction at the lattice.

2.7.2 Intensity calculation

The (theoretical) intensity is proportional to the square of the amount of the structure factor of the reflection. The proportionality factor includes the original intensity I_0, the wavelengths of the primary beam λ and correction factors. The absorption factor takes into account that a part of the X-rays is absorbed and thus not diffracted. The Lorentz factor takes into account that in moving crystals, reflections with higher diffraction angles remain in the reflection position longer than those with lower angles. Due to the movement apparently the intensity of the higher diffraction angles increases. The polarization factor takes into account that the amplitude of the scattered radiation is proportional to the sine of the angle between the orientation of the electric vector of the incident and scattered radiation. This is important for unpolarized X-rays. The extinction factor accounts for the fact that as the penetration depth increases, the radiation is attenuated by Bragg scattering. The area frequency factor takes into account the exaggeration of the intensity of a reflection, since several mesh plane arrays with the same Mitterian indices are simultaneously in the reflection position.

2.7.3 Temperature factor

The temperature factor takes into account the increase in the deflections of the oscillations of the atoms about their equilibrium position with increasing temperature. The increase of the oscillations leads to a decrease of the scattering force and the intensities of the reflections.

2.7.4 Background in a Powder diffractogram

The background comes from extraneous wavelength components of the monochromatic X-rays. Foreign bodies in the beam path or the sample are also part of the background. At smaller angles, even small deviations in the wavelength can cause reflections to occur further than at larger angles.

3 Methods and Materials

3.1 Setup for X-ray Absorption Measurement

To measure the emission spectrum of the anode, a setup as shown in Fig. 3.1 is used. The X-rays are generated in an X-ray tube (RR). A monochromator, realized in a rotatable single crystal (K), selects a specific wavelength of the X-ray spectrum depending on the angle 2θ set. After an aperture (B), the now nearly monochromatic X-ray radiation hits the sample holder (F). Into this holder the sample can be inserted. After the radiation passed the sample holder, the intensity of the radiation is measured by a counting tube (Z) and the data is transferred to a computer.[2]

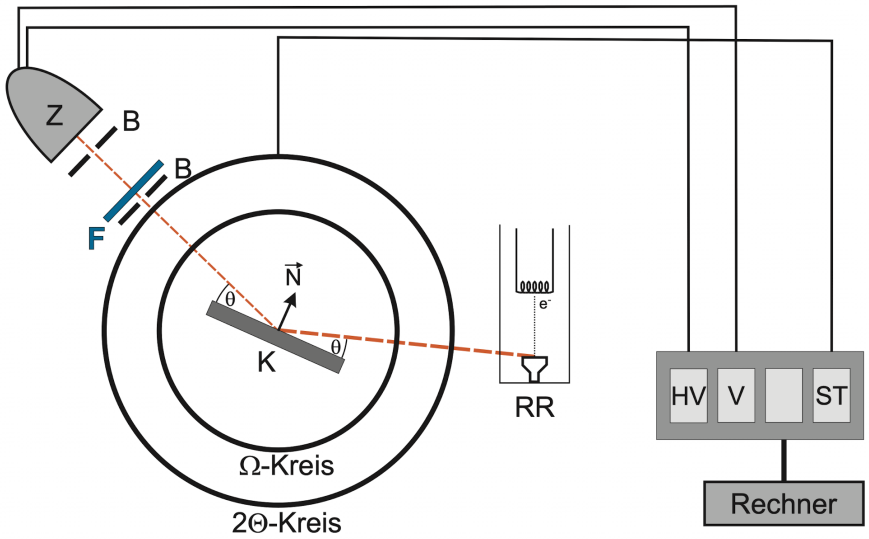

Figure 3.1: Experimental setup of the absorption measurement.[2]

3.2 Setup for Diffraction Measurement

For the diffraction measurement we are using a similar setup to the setup used before. As depicted in Fig. 3.2, the X-rays are generated in an X-ray tube (RR). Afterwards a monochromator selects one X-ray wavelength. The sample (S) is turned as the single crystal in the absorption setup. For each position the diffraction under 2θ is measured by a counting tube (Z) and the data is transferred to a computer.

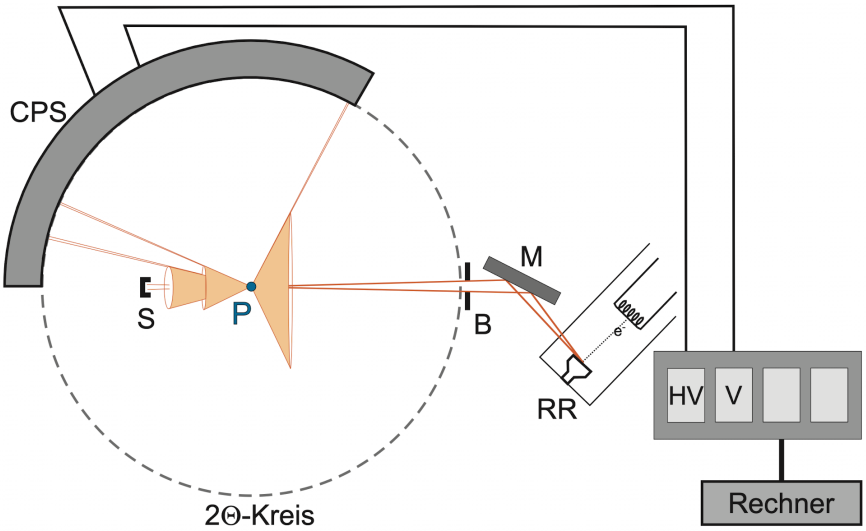

Figure 3.2: Experimental setup of the diffraction measurement.[2]

In the sample preparation procedure, the crystal under examination (e.g., NaCl, glucose) is finely ground using a mortar. The resulting powder should possess a fine texture, barely detectable when rubbed between the fingers. Subsequently, the powder is carefully loaded into a sample holder, paying attention to a flat surface of the powder. Finally, the sample holder is inserted into the X-ray setup and the measurement is started. The measurement process runs for approximately one week.[2]

4 Evaluation

4.1 Identification of Metal Foils by their Absorption Edges

In the following section, we are going to identify an unknown metal foil due to its absorption edges. The used setup is described in Chapter 3.1. The setup is able to measure the transmitted intensity in regard to a diffraction angle. The measured angle $\omega = 2\Theta$ can be varied from $5.0° \leq \omega \leq 51.0°$ with a step width of $0.1°$. In the beam path, we placed three foils marked with an index 2, 3, 4 of thickness $d_\mathrm{f} = 2.5 \cdot 10^{-5}\,\mathrm{m}$. A reference measurement was performed as well.

4.1.1 Calibration of the Device

First step is to calibrate the machine to evaluate the correct data from the measurement. For this we use the known characteristic radiation of our Tungsten anode. The sharp peaks should be visible in the X-Ray intensity spectrum if they fulfill the Bragg condition

$$2d \sin\omega = n\lambda \ , \tag{4.1}$$

with ω being same angle mentioned above, λ being the wavelength of the spectrum, n the oder of diffraction and d being the grid plane spacing. For the cubic CaF_2 crystal, which is used in this experiment as reference, the grid plane distance can be calculated as

$$d_{hkl} = \sqrt{\frac{a^2}{h^2 + k^2 + l^2}} \ , \tag{4.2}$$

with $(hkl) = (220)$ being the Laue indexes and $a = (5.463 \pm 0.001)\,\text{Å}$. Therefore, $d = (1.9314 \pm 0.0004)\,\text{Å}$ in this geometry. Since the errors are very small, they will be neglected for the rest of the evaluation. To calculate the angle of Equation (4.1) gets rearanged for the angle ω as following

$$\omega = \arcsin\left(\frac{n\lambda}{2d}\right) \ . \tag{4.3}$$

Assuming the dominant peaks for lower angle are peaks due to the first order of the diffraction ($n = 1$), we correlate those with the known peaks from Ref. 2. The smaller

one are correlated to the second order of diffraction ($n = 2$). The theoretical values for the characteristic peaks of the wolfram anode are from *National Institute of Standards and Technology*. Transforming the theortical peak values given in λ into angles in our geometry Θ and taking into account their relative intensity, the peaks are identifiable as the peaks of the *Lyman series*. To calibrate our device, we assume linear scale with

the parameters: t as offset and m as slope. Therefore, we fit a straight line to our data Θ_{Data} plotted against the theoretical values Θ_{Theo} for the first and second order together with the following equation

$$\Theta_{\text{Theo}} = m * \Theta_{\text{Data}} + t \ . \tag{4.4}$$

The fit can be seen in Fig. 4.1. Calculation yields following result

$$\boxed{m = 0.996 \pm 0.002 \qquad t = (0.284 \pm 0.035)^\circ} \ .$$

These two parameters will be used to calibrate our device from now on. In Fig. 4.2 one can see the correctness of the calibration for the frist order and second order diffraction peaks.

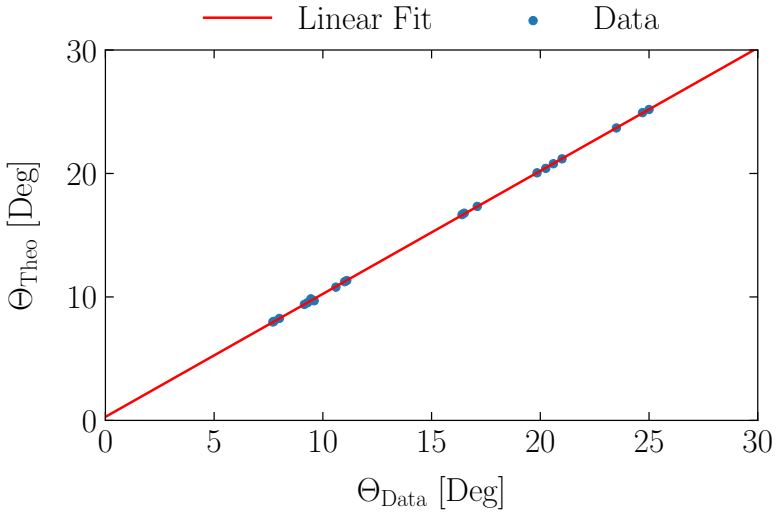

Figure 4.1: The extracted peaks Θ_{Data} are compared to the theoretical values Θ_{Theo} and are fitted with a linear fit function. Note that the fit was performed for first and second order peaks together.

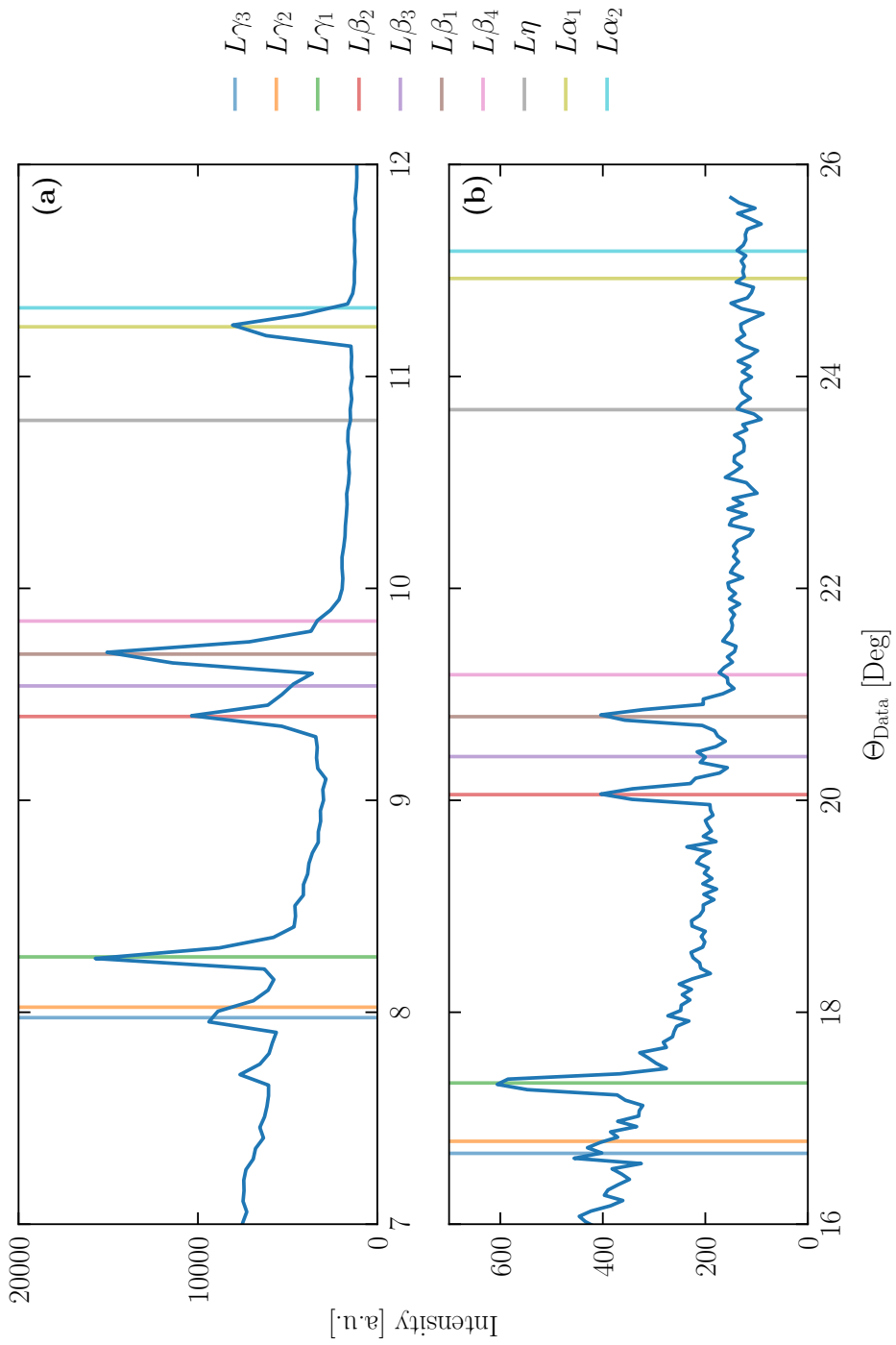

Figure 4.2: Corrected X-Ray spectrum of the device with the theortical values of the peaks named in Siegbahn notation. In (a) the peaks of first order are displayed and in (b) the peaks of second order.

4.1.2 Identification of Metal Foils

In this section we want to identify the type of metal for foil 2, 3, 4. When a metal is irradiated with X-Rays, strong, irregular absorption bands become visible. These are created when the electrons exceed a certain energy form, they can interact and free electrons from lower energy levels of the atom. This leads to a sharp jump in the absorption. The mass attenuation coefficient μ/ρ is from special intrest. It can be derived from the Lambert-Beer Law and is given by

$$\frac{\mu}{\rho} = \frac{1}{\rho d_\mathrm{f}} \log\left(\frac{I_0}{I}\right) , \tag{4.5}$$

with the density ρ and the thickness of the foil d_f. The specific energy at which those jumps take place depend on the internal energetically structure of the atom, especially on the number of protons. Therefore, it is possible to distinguish the different metals. The different X-Ray absorption spectrums for each foil are shown in Fig. 4.3 with transfromed angle Θ into wavelength λ under the use of Equation (4.1) with $n = 1$.

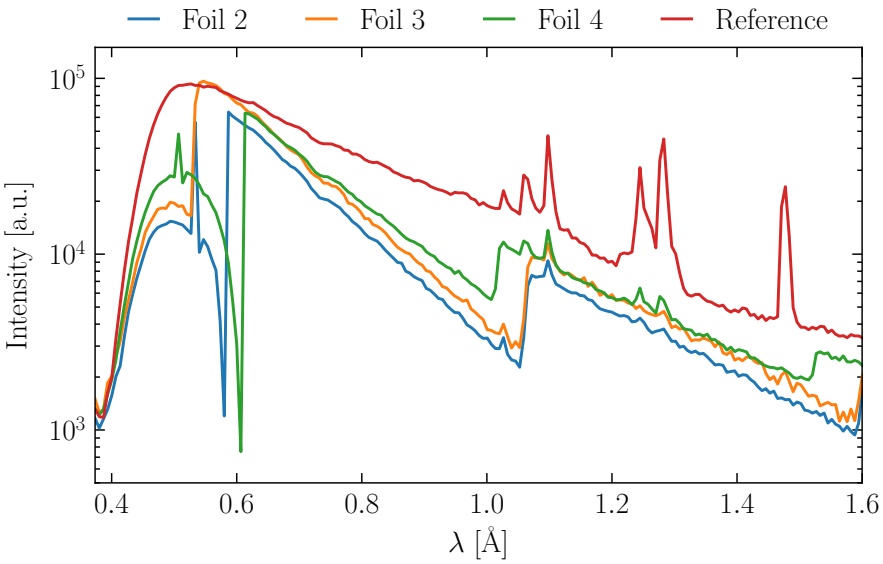

Figure 4.3: X-Ray intensity spectrum of foil 2, 3 and 4 plotted against the reference signal with logarithmic y axis. The reference signal and the signal of foil 3 was shifted in height to achieve alignments.

A closer look at the first sharp jump in the spectrum yields following result with the comparison from the *National Institute of Standards and Technology*[1]

- **Foil 2**: 0.585 Å ⇒ Pd (Palladium) (or Np (Neptunium)),
- **Foil 3**: 0.530 Å ⇒ Rh (Rhodium) (or Cf (Californium)) and
- **Foil 4**: 0.610 Å ⇒ Not exactly determinable.

In the case of foil 4 it is not clear from the database which metal foil 4 contains. In the range of the evaluated value one can only find elements which are radioactive, so we assume a measurement error occurred. The frist sharp edge of each foil is displayed in Fig. 4.4. For the other foils the result is also too inaccurate to determine the right metal.

Since the evaluation of the first sharp jump does not yield exact results, no further evaluations will be performed.

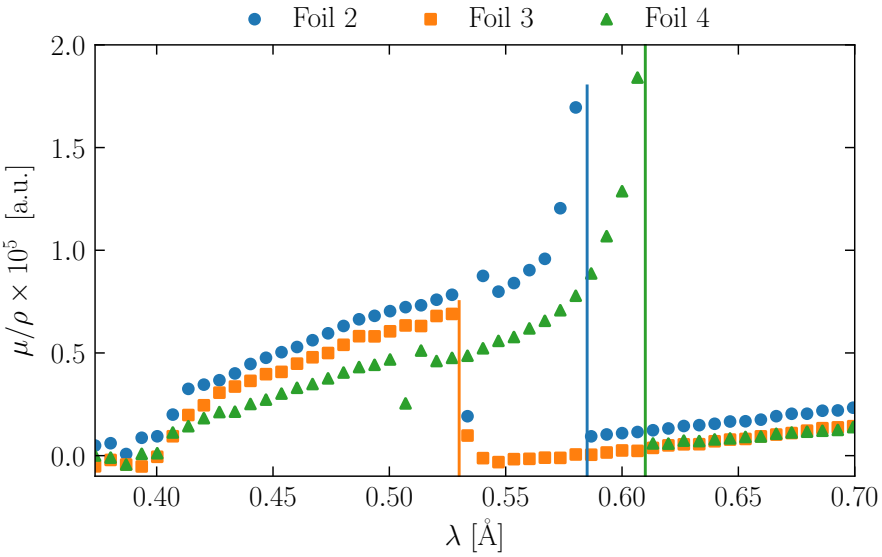

Figure 4.4: The absorption takes a sharp jump for the foil 2 close to $\lambda = 0.585\,\text{Å}$, for foil 3 close to $\lambda = 0.530\,\text{Å}$and for foil 4 close to $\lambda = 0.610\,\text{Å}$.

4.2 Crystal Structure of Sodium Chloride (NaCl)

Structural Analysis

The following section, we are going to examine the structure of NaCl, the plot shows the obtained intensity distribution.

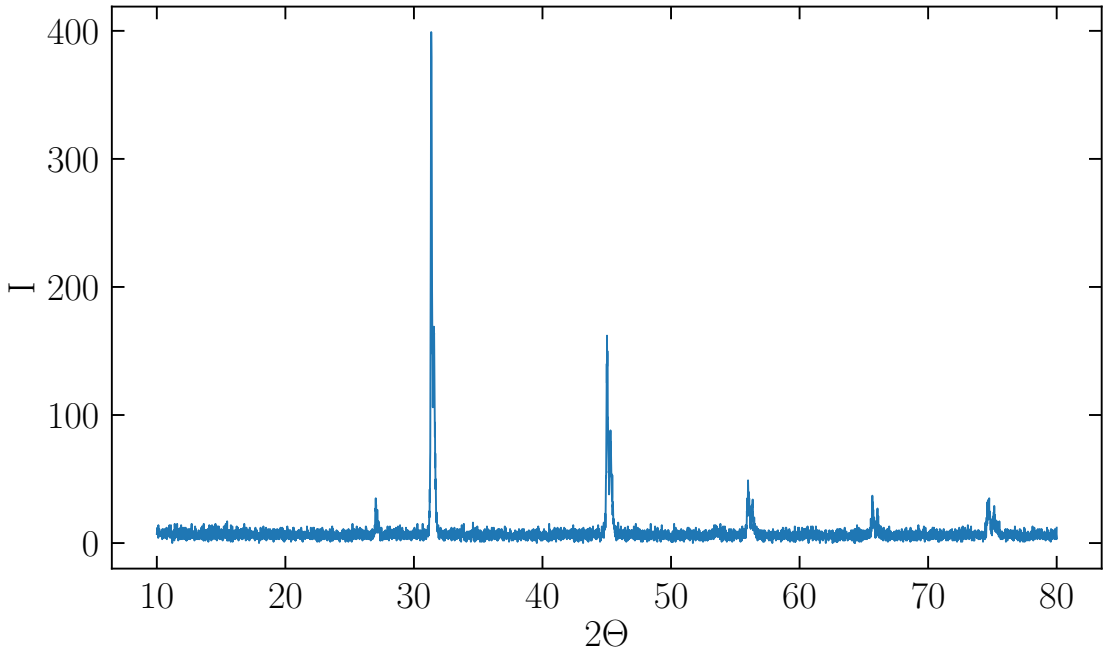

Figure 4.5: Intensity distribution of the NaCl experiment.

The following table shows the intensity, the full width at half maximum (FWHM) and the positions of each peak.

Peak No.	$2\theta_{fit}$ / ř	I_{fit} / a.u.	$FWHM$ / ř
1	27.15	0.05	0.11
2	31.48	0.86	0.12
3	45.02	0.48	0.16
4	53.62	0.03	0.18
5	56.21	0.15	0.19
6	65.66	0.10	0.22
7	72.70	0.02	0.24
8	74.70	0.17	0.25

Table 4.1: Fit values for each peak in the intensity distribution.

Using the following realtions:

Bragg condition:

$$2dsin(\Theta) = m\lambda \tag{4.6}$$

Distance between to planes in a cubic system:

$$d = \frac{a^2}{h^2 + k^2 + l^2} \tag{4.7}$$

with the laue indices h, h, l and the lattice parameter a.
In the following we assume $m = 1$. So we can derive the following equation:

$$sin^2(\Theta) = (h^2 + k^2 + l^2)\frac{\lambda^2}{4a^2} \tag{4.8}$$

We define the constant: $c^{-1} = \frac{\lambda^2}{4a^2}$, which depends only on the setup.
We can write an equation to compute a:

$$a = \sqrt{c}\frac{\lambda}{2} \tag{4.9}$$

Using this relations and the date from table 4.1 we get the values displayed in the following table (table 4.2):

Peak No.	$2\theta_{fit}$ / ř	d / Å	$\sin^2(\theta)$	$\frac{\lambda^2}{4a^2}$	$h^2 + k^2 + l^2$	a / Å	(h k l)
1	27.15	3.28	0.055	0.018	3	5.682	(1 1 1)
2	31.48	2.84	0.074	0.018	4	5.677	(0 0 2)
3	45.02	2.01	0.147	0.018	8	5.689	(2 0 2)
4	53.62	1.71	0.203	0.018	11	5.662	(1 1 3)
5	56.21	1.63	0.222	0.018	12	5.662	(2 2 2)
6	65.66	1.42	0.294	0.018	16	5.681	(0 0 4)
7	72.70	1.30	0.351	0.018	19	5.663	(3 1 3)
8	74.70	1.27	0.368	0.018	20	5.676	(2 0 4)

Table 4.2: Lattice parameters and indices for each peak fitted.

On average, the lattice parameter is $a = 5.674$. This fizs pretty well with the literature value os $a = 5.64$ (Wikipedia).

4.3 Crystal structure of Zircon/Zirconium(IV)silicate (ZrSiO4)

Using the Rietveld-wizard from Jana2006 we do the peak profilingand get the profile showed in figure 4.6 and the parameters:

$$a = b = 6.608\,\text{Å} \quad c = 5.988\,\text{Å} \tag{4.10}$$

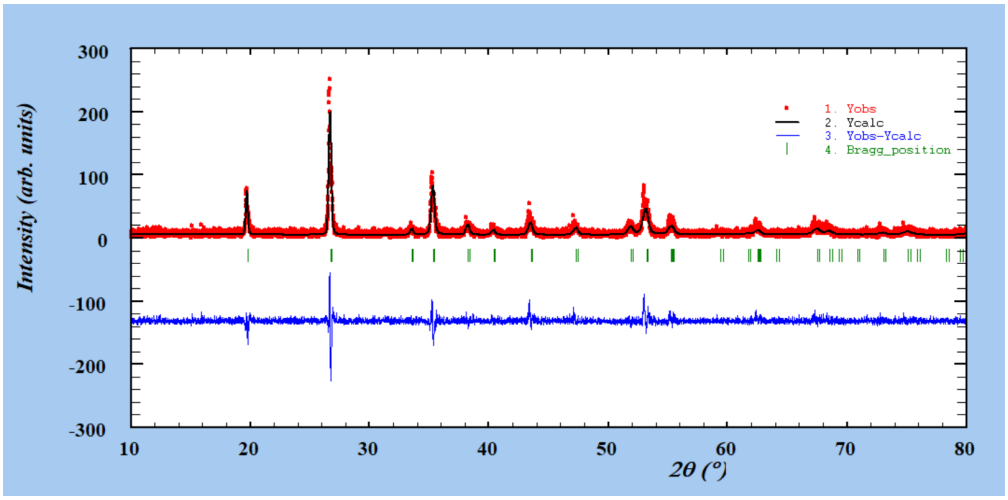

Figure 4.6: Resulting profile

Te difference plot shows some peaks, which are due to inaccuracies.

Furthermore, the structure shown in figure 4.7 were generated via Jana2006.

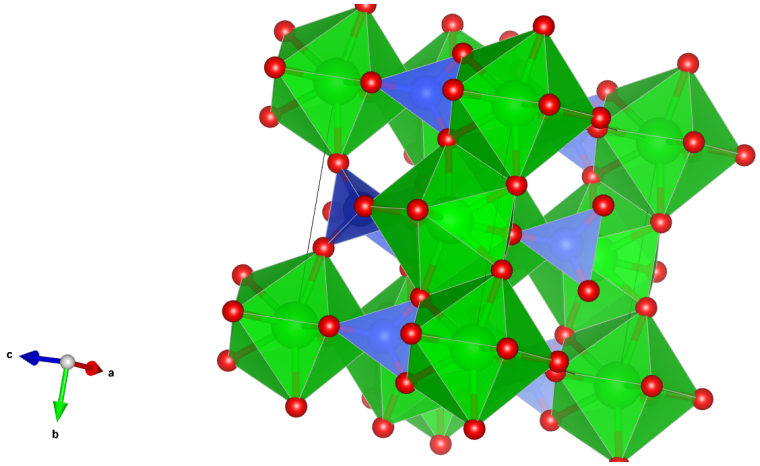

Figure 4.7: Structure model in polyhedral style. ZrO_8 trigondodecahedra in green and SiO_4 tetrahedra in blue.

5 Closure

Finally, thanks to this experiment, we got an insight into the basics of structure analysis with X-rays.

Bibliography

[1] of Standards, National Institute & Technology ???? X-ray transition database. https://physics.nist.gov/cgi-bin/XrayTrans/search.pl?element=All&trans=All&lower=0.5&upper=0.65&units=A. Accessed: 2023-08-01.

[2] Versuchsanleitung 2015 Laser. Internes Dokument, Universität Bayreuth.